



## Research articles

## Novel applications of magnetic materials and technologies for medicine

V.I. Zverev<sup>a,\*</sup>, A.P. Pyatakov<sup>a</sup>, A.A. Shtil<sup>c</sup>, A.M. Tishin<sup>a,b</sup><sup>a</sup> M.V. Lomonosov Moscow State University, Leninskie Gori, Moscow 119991, Russia<sup>b</sup> Pharmag LLC (AMT&C Group), 142190 Troitsk, Moscow, Russia<sup>c</sup> Blokhin Cancer Center, 24 Kashirskoye Shosse, Moscow 115478, Russia

## ARTICLE INFO

## Article history:

Received 10 July 2017

Received in revised form 5 October 2017

Accepted 7 November 2017

Available online 8 November 2017

## ABSTRACT

We analyze the applications of the magnetocaloric effect (MCE) achieved with advanced magnetic materials and technologies. New results such as the use of MCE-based composite material for ‘smart’ coating of implants, which allows for a controlled release of drugs over time. The material is comprised of two layers: the one manifesting a large MCE and the other made of a temperature-responsive polymer containing the drug. The latter is released by the polymer if the temperature induced by magnetic field (due to MCE) is changed. The polymer undergoes sharp phase transition in response to the slight temperature drop of  $\sim 1\text{--}3\text{ }^{\circ}\text{C}$  (down to  $34\text{--}36\text{ }^{\circ}\text{C}$  in the body). Local cooling is achieved with FeRh alloy, one of the most perspective MCE materials with the first order phase transition. It is critically important to take into account several peculiarities of phase transition and MCE behavior in these series of alloys. Recent studies on high-purity samples showed an ‘irreversible’ effect of MCE indicating that the temperature of FeRh does not return to its initial value after the full cycle of the magnetic field during dynamic MCE measurements. A theoretical explanation based on *ab initio* calculations has been provided. Magnetic hyperthermia in oncology is rapidly developing therapeutic modality. Recent experiments have shown that Mn-Zn ferrite emerges as a cost-effective material for this method compared with currently used magnetite nanoparticles. We present our achievements on magnetically guided capsule endoscopy. The advances in magnetically guided capsule endoscopy are also discussed. We provide the experimental setup for the computer-controlled system of magnetic field sources that create necessary forces to control the position of the capsule in five degrees of freedom in a given area. The system has the feedback on the position and is designed to monitor the endoscopic capsule during gastrointestinal tract examination.

© 2017 Elsevier B.V. All rights reserved.

## 1. Introduction

Currently the ‘boom’ in research activity is directed to a traditional magnetic hyperthermia utilizing magnetic nanoparticles with close to zero value of the magnetocaloric effect (MCE). This effect can be accomplished using magnetic refrigeration and magnetocaloric hyperthermia technologies [1,2]. Despite the efforts to develop a commercially available prototype of magnetic refrigerators these attempts have not yet led to a wide spread of this technology mainly due to the cost of the magnetic field source. In the same time, MCE has a potential of being used for magnetocaloric hyperthermia and drug delivery. The endoscopic capsule, micro-robotics and other techniques based on the controlled localization of the object by the magnetic field have been considered in clinical oncology. We herein describe our recent progress in these directions.

## 2. MCE-based composite material: ‘smart’ coating for drug delivery

The MCE-based composite material for smart coating of implants is perspective for release of entrapped drugs over time in controlled amounts has been recently internationally patented see international patents in Refs. [3,4]. We developed a magnetic field based controllable device capable of retaining biologically active substances *in situ*. A pulsed field allows for a temporary drug release and avoidance of device overheating or insufficient heating.

The implantable device consists of:

- first heat-insulating layer
- a layer of magnetic material having positive or negative magnetocaloric effect of at least 3 K/T
- a layer of a sensitive material comprising the active substance for controlled retention/release.
- second insulator layer permeable for the active substance.

\* Corresponding author.

E-mail address: [vi.zverev@physics.msu.ru](mailto:vi.zverev@physics.msu.ru) (V.I. Zverev).

The thermodynamic model of the implant consisting of the magnetocaloric material and the polymer gel implies the solution of heat conduction equation:

$$\frac{\partial U}{\partial t} = \frac{\kappa}{C\rho} \frac{\partial^2 U}{\partial x^2}, \tag{1}$$

where  $U(x, t) = T(x, t) - T_0$  is the temperature distribution defined as a difference between the local temperature and the body temperature  $T_0 = 37^\circ\text{C}$ ,  $\kappa$  is heat conduction constant,  $C$  is heat capacity,  $\rho$  is the density of the medium.

Representing the solution as a Fourier series of spatial harmonics  $q_n$ :

$$U = \sum_n A_n \cos(q_n x) \cdot e^{-\frac{\kappa}{C\rho} q_n^2 t}$$

one can find the characteristic thermodynamic equilibrium time as:

$$\tau_0 = \frac{C\rho}{\kappa q_1^2}$$

Comparison of the thermodynamic equilibrium time with other constants such as characteristics of MCE (spin-lattice relation time) and the gel swelling time is shown in Fig. 1. For an interstitial fluid with parameters close to water:  $\kappa = 0.56 \text{ W/(m K)}$ ,  $C = 4200 \text{ J/(kg K)}$ ,  $\rho = 1 \text{ g/cm}^3$  this time for  $60 \mu\text{m}$  layer will be of an order of one millisecond that is much higher than spin-lattice relation time  $\sim 100 \text{ ps}$  but much shorter than the gel swelling time  $\sim 0.3 \text{ s}$  (estimated by scaling the collapse time of  $100 \text{ nm}$  particles  $360 \text{ ns}$  to  $100 \mu\text{m}$  range, taking into account the diffusion scaling law  $\tau \sim l^2$  [5]). To obtain the final temperature  $32^\circ\text{C}$   $\Delta T_\infty = -5\text{K}$  in the entire volume of the polymer layer using  $60 \mu\text{m}$  film of FeRh with specific heat capacity  $C = 300 \text{ J/(kg}\cdot\text{K)}$ , and density  $\rho = 10 \text{ g/cm}^3$  one have to provide the initial temperature drop  $\Delta T = -13^\circ\text{C}$  achievable in 2 Tesla magnetic field.

Local cooling is achievable with FeRh alloy, one of the most perspective MCE materials with the first order phase transition. It is critically important to take into account several peculiarities of phase transition and MCE behavior in these alloys [6]. Recent studies with high purity samples showed an ‘irreversible’ effect of MCE indicating that the temperature of FeRh does not return to its initial level after the full cycle of the magnetic field during dynamic MCE measurements. A theoretical explanation based on *ab initio* calculations has been provided [6]. See Fig. 2.

We assumed that the sample had tiny fluctuations in its composition, so it comprised many regions characterized by slightly different values of long range order,  $S = 1 - y$ , close to one.

These experimental results have been theoretically described by an *ab initio* disordered local moment theory model [6].

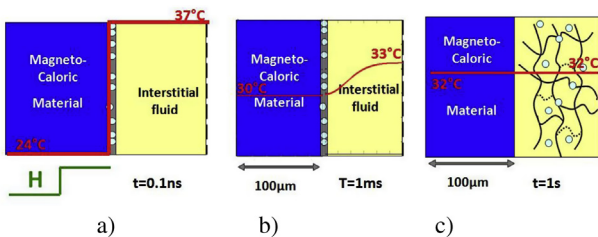


**Fig. 1.** Stages: a) spin relaxation in the magnetocaloric material; b) heat diffusion process in the interstitial fluid; c) swelling of the polymer. The red line corresponds to the spatial temperature distribution. Blue circles are drug particles within the collapsed polymer layer (Fig. 1a, b) and distributed in the polymer mesh (swelled state; Fig. 1c). (For interpretation of the references to colour in this figure legend, the reader is referred to the web version of this article.)

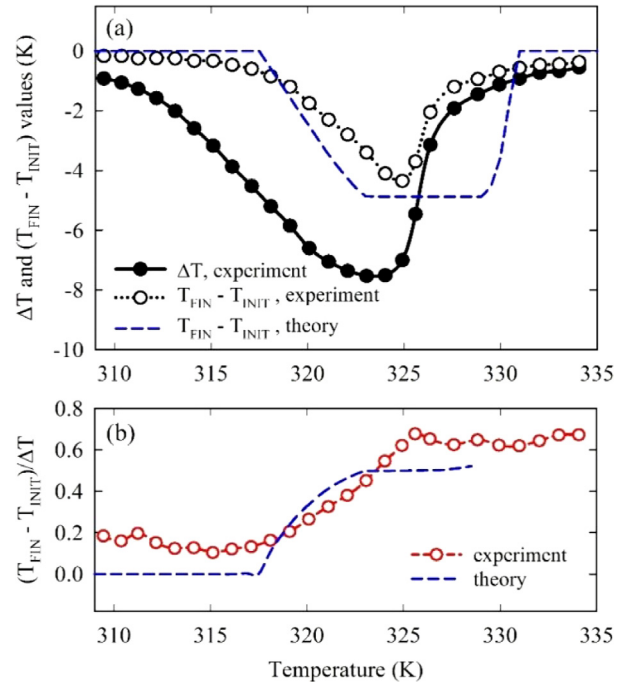


**Fig. 2.** Temperature dependence of (a) absolute (open circles) and (b) relative values of  $(T_{\text{FIN}} - T_{\text{INIT}})$  for  $\text{Fe}_{50.4}\text{Rh}_{49.6}$  from both experiment and theory. The plot (a) also shows the experimental  $\Delta T(T)$  dependence for comparison of peak positions [6].

It has been shown that slight variation from complete compositional B2 order and small compositional inhomogeneities significantly influence both the AFM-FM phase transition temperature and the behavior of the temperature dependence of magnetocaloric properties.

Comparison of theoretically determined and experimentally measured MCE values supported the theoretical conclusion about a large electronic contribution (up to 40%) during AFM-FM transition in FeRh alloys.

Preclinical testing started with the mesh implants used as the surgical materials (Fig. 3). The original layer by layer (LbL) method of  $\text{Fe}_3\text{O}_4$  magnetic nanoparticle deposition on polypropylene and polyvinylidene fluoride was developed. The procedure of LbL coating is based on electrostatic attraction of layers.



**Fig. 3.** Samples of mesh implants. The coating of magnetic nanoparticles and tungsten nanoparticles (LbL deposition method) (see text for details).

First, a layer of the gel formed by positively charged polyelectrolyte (polyallylamine hydrochloride) is placed on the surface of polypropylene and polyvinyl difluoride. The surface is then washed with distilled water followed by adsorption of negatively charged magnetic nanoparticles on top of the surface and washing with water.

### 3. Magnetic hyperthermia

This treatment modality gains momentum as a well tolerable and efficient approach in adjunct to conventional chemo- and radiotherapy. The antitumor magnetic hyperthermia is based on the direct introduction of magnetic materials into the tumor region and subsequent heating. The magnetic fluid based on iron oxide ( $\text{Fe}_3\text{O}_4$ ) nanoparticles coated with aminosilane or dextran is used as a magnetic-field-induced heating material. Depending on the tumor size and location the frequency of the external magnetic field varies from 1 kHz to 1 MHz.

We developed the first acting prototype of the magnetic field source for air-cooled experiments. The active volume of the magnetic field coil has an internal diameter of 50 mm and a height of 80 mm. The amplitude and frequency of the alternating field are 100 Oe and 100 kHz, respectively.

The experimental setup (Fig. 4) includes: 1) a system for creating a magnetic field, including power sources, a generator and a magnetic coil (solenoid), as well as the control circuits; 2) a temperature measuring system consisting of a thermocouple and a measuring voltmeter; 3) a cooling system consisting of a coil water

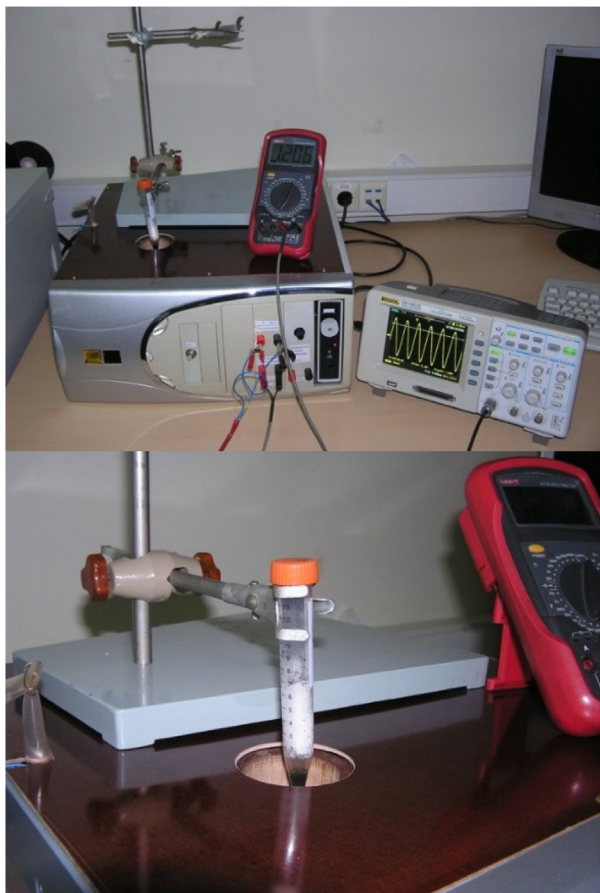


Fig. 4. Experimental setup for measurements of heating of magnetic particles in AC magnetic field. The magnetic field generator module is jacketed in PC desktop tower. The test tube is placed into the 50 mm hole of the solenoid.

cooling device and additional cooling fans of the generator and a power source; 4) an external control system that includes a personal computer and a switching device.

The system for creating the magnetic field consists of a power source, a generator and a magnetic coil (solenoid). Voltage from the network decreases by the power source and enters the generator. The latter provides the signal in the solenoid with a frequency of 100 kHz. This makes it possible to achieve a magnetic field of 100 Oe in the working aperture of the coil.

The temperature dependences of heating temperature over time for the following compositions of nanoparticles were measured: magnetite  $\text{Fe}_3\text{O}_4$ , lanthanum-strontium manganite ( $\text{La}_x\text{Sr}_{1-x}\text{MnO}_3$ ), zinc-ferrite manganese ferrite  $\text{Zn}_x\text{Mn}_{1-x}\text{Fe}_2\text{O}_4$  (Fig. 5) [7]. Average particle size for these samples was 10–50 nm. Samples containing 20 mg of nanoparticles of different composition were prepared by dispersing the substances in 100  $\mu\text{l}$  of distilled water.

Specific heating power was calculated for the best samples of different chemical composition using the formula:

$$\text{SAR} = C \frac{dT}{dt} \frac{M}{m}$$

where C is the heat capacity of water,  $dT/dt$  is the heating rate at the initial section of the curve,  $M/m$  is the ratio of the mass of heated water to the mass of particles (Table 1).

Thus,  $\text{Zn}_{0.1}\text{Mn}_{0.9}\text{Fe}_2\text{O}_4$  was selected for further analysis of the heating mechanism. In so doing the time course of final temperature was measured, and specific heating power SAR for different values of the field amplitude was calculated. Since the process is not adiabatic, both heating and cooling curves were measured (Fig. 6).

The values of the intrinsic loss of power  $\text{ILP} = 121 \pm 3 \text{ nH m}^2/\text{kg}$  remain constant within the error margin for all field amplitudes. Hence, we conclude that, for these nanoparticles, the dependence of heating on the field is close to quadratic, and the dominant mechanism for heating nanoparticles in an alternating magnetic field is Neel relaxation, which is characteristic of the magnetization reversal of superparamagnetic particles in the absence of Brownian relaxation due to mechanical rotation and losses due to hysteresis.

An additional confirmation of the relaxation mechanism of heating is the quadratic dependence of the heating power on the field amplitude.

In order to test the efficacy of the selected manganese ferrite composition, the K562 human myeloid leukemia cell line was heated in the presence or absence (mock; control) of 10 mg of zinc-substituted manganese ferrite for 60 min followed by incubation for 24 h at 37 °C, 5%  $\text{CO}_2$  in a humidified atmosphere. Only a few cells remained visible after heating in the presence of the new material (Fig. 7left) whereas control cells proliferated

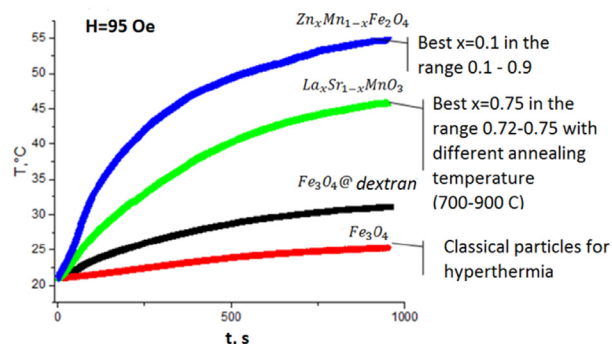
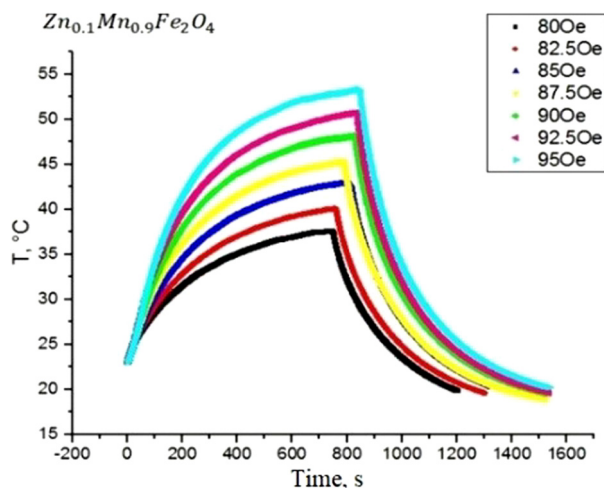


Fig. 5. Time dependence of temperature for magnetic nanoparticles of various chemical compositions in response to 100 kHz AC magnetic field [7,8].

**Table 1**

Values of specific heating power for the best samples of individual chemical compositions.

Sample (20 mg + 100 $\mu$ l water)	SAR, W/g
$\text{Fe}_3\text{O}_4$	$0.11 \pm 0.02$
$\text{Fe}_3\text{O}_4$ (dextran coated)	$0.63 \pm 0.09$
$\text{La}_{0.75}\text{Sr}_{0.25}\text{MnO}_3$	$1.5 \pm 0.2$
$\text{Zn}_{0.1}\text{Mn}_{0.9}\text{Fe}_2\text{O}_4$	$3.1 \pm 0.2$



**Fig. 6.** Time dependence of temperature for different values of the amplitude of the 100 kHz AC magnetic field for zinc-ferrite manganese ferrite nanoparticles. At 800 s the AC field was switched off (cooling) [7].

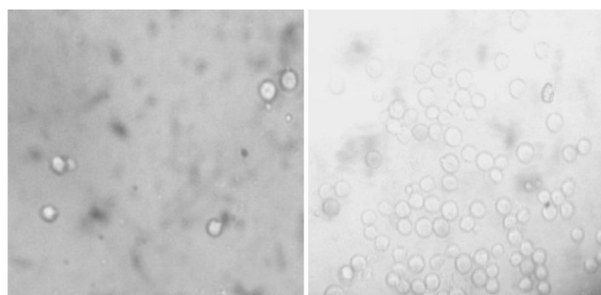


**Fig. 7.** (left) Microscopy of K562 cells heated in the presence of 10 mg  $\text{Zn}_{0.1}\text{Mn}_{0.9}\text{Fe}_2\text{O}_4$  (24 h post heating). (right) Mock-heated K562 cells [7].

(Fig. 7right). These results demonstrated the cytotoxic potency of magnetic fluid hyperthermia.

#### 4. Magnetically guided capsule endoscopy

The original wireless capsule endoscopy (WCE) is a medical screening method in which a small capsule is swallowed and transported along the gastrointestinal tract by physiological peristalsis. The capsule has one or more cameras to take images that are sent wirelessly and stored in a portable receiver. The images are extracted after the capsule has passed through the small intestine and viewed and analyzed on a workstation. WCE allows to screen broad population cohorts. This method can be used for identifying the bleeding vessels, for diagnosis of Crohn disease, benign and malignant intestinal tumors.

The major concept of the capsule endoscope has not changed much over the years. Typically the outer shell consists of a

bio-compatible polycarbonate with a transparent end as a half-sphere which covers the imaging sensor and multiple LEDs on a round circuit board. Behind it is a connected ASIC for signal processing and control of the radio transmitter unit next to it. The radio signal is transmitted on the ISM band (Industrial, Scientific and Medical Band, 433.05–434.79 MHz). The power is provided by one or more button cells whose rounded structure fits inside the capsule shell. Flexible flat cables connect the components. The size of the capsules is  $\sim 36$  mm in length and 11 mm in diameter.

Having only one camera the orientation of the capsule's view in the intestine is not necessarily forward. It is not important which direction the capsule is facing because of the hollow pipe-like form of the intestine. Studies have showed that the capsule is actually not constant in its facing direction and will often unpredictably turn around its diagonal axis. This raised a concern that the capsule endoscopy does not guarantee a reliable diagnosis. Direct solution of this problem does not exist, but very wide viewing angles of the cameras allow for reasonable observing. Olympus and Given Imaging have introduced wider angles with the newest versions of their capsules. There are capsules available with two cameras, but these are designed for different applications. The PillCam COLON by Given Imaging is applicable for the colon, and PillCam ESO for the esophagus examinations. A capsule with four cameras is available from CapsioVision4 that has fully transparent shell (cameras are arranged in the center facing four directions).

Two major problems remain unsolved: the miniaturization and the power consumption of the locomotion mechanism. To address the power consumption problem a promising approach is not to carry the necessary energy inside the capsule or microrobot but to use an external power source. An inductive wireless power transmission is one solution, but the coils necessary to receive the power come with constraints for the size and weight of the capsule.

An alternative are magnetically generated forces. With the magnetic field outside the patient body the translational and rotational forces can act on permanent magnets or magnetizable materials of any size. Minimally invasive methods in gastroenterology which make use of magnetism are almost exclusively based on further advances of capsule endoscopes. Important works in this field have been discussed in our publication [9].

The work of Pharmag LLC was aimed at simultaneous optimization of the mass-size, energy and cost characteristics of systems for



**Fig. 8.** Acting prototype of electromagnetic system for control of endoscopic capsule designed by Pharmag LLC (AMT&C Group), Russia [10].

monitoring the positioning of the capsule inside the body with the help of an external magnetic field. The created prototypes allow to control the movement and angular orientation of the capsule by the effect of the external field in a volume of 200 mm in diameter. In Fig. 8 the acting prototype of the electromagnetic system is presented (patent application is pending) [9].

The prototype has 8 electromagnetic coils and uses feedback based on high-resolution optical cameras. The electromagnetic system makes it possible to create a necessary magnetic field gradient at each point of the internal space to control the 5 capsule DoF in an aquarium 10x10x10 cm with water and is controlled by a wireless joystick, providing computer control of the current in each of the coils.

## 5. Conclusion

In our opinion, the community of magnetocalorimetry scholars should consider possible medical applications for marketing. These applications are less demanding in terms of the cost of materials (FeRh alloy with the biggest MCE value achieved so far [11] can be used). It is possible to use the magnetic field of MRI equipment thereby eliminating the problems of magnetic refrigerators that limit the entry to the market. Also, an integrated approach is required that allows not only to heat the tumor but also to deliver drugs to the site. The endoscopic capsule can be used for point-to-point targeted delivery of nanoparticles and chemicals in gastrointestinal cancer.

## Acknowledgements

The authors are thankful to Prof. Julie B. Staunton and Dr. Henrik Keller for productive discussions, to Prof. Yu. Gun'ko, Dr. D. Kopeliovich, R. Salakhova, Dr. R.Gimaev, A. Malyshev, S. Goncharov, V. Markov, Dr. A. Markova and A. Kritskiy for assistance in experiments. The authors thank the Ministry of Science and Education of Russia for financial support of the work (Federal target program "Research and development in priority areas of development of Russia's scientific and technological complex for 2014–2020", grant identification RFMEFI60417X0197).

## References

- [1] A.M. Tishin, Y.I. Spichkin, V.I. Zverev, P.W. Egolf, *Inter. J. Refrig.* **68** (2016) 177–186.
- [2] A.M. Tishi, European patent, 1 897 590, B1 (2016).
- [3] A.M. Tishin, A. Rochev Yu, A.V. Gorelov, US patent 9,017,713, B2 (2015).
- [4] Y.I. Spichkin, A.P. Pyatakov, A.M. Tishin, V.I. Zverev, GB patent, 2520960 (2015).
- [5] Z. Ahmed et al., *J. Phys. Chem. B* **113** (2009) 134248–134256.
- [6] V.I. Zverev, A.M. Saletsky, R.R. Gimaev, A.M. Tishin, T. Miyanaga, J.B. Staunton, *Appl. Phys. Lett.* **108** (2016) 192405.
- [7] A.M. Tishin, A.P. Pyatakov, A.A. Shtil, Gun'ko Yu., V.I. Zverev, R.T. Salakhova, A. A. Markova, Application number 2016112370, Dated 01.04.2016.
- [8] R.T. Salakhova, A.A. Markova, *Materialy Mezhdunarodnogo molodezhnogo nauchnogo foruma Lomonosov -2016*, p. 195 (in Russian).
- [9] N. Shamsudhin, V.I. Zverev, H. Keller, S. Pane, P.W. Egolf, B.J. Nelson, A.M. Tishin, *Med. Phys.* (2016), accepted for publication.
- [10] A.M. Tishin, D.B. Kopeliovich, L.V. Dolgov, A.A. Kritskiy, D.A. Demesh, Equipment for control of movement of foreign body inside the patient by external magnetic field, Application number 2017118208, Dated 25.05.17.
- [11] S.A. Nikitin, G. Myalikgulyev, A.M. Tishin, et al. *N 6,7 Phys. Lett. A* **148** (1990) 363–366.